ELSEVIER

Journal of Alloys and Compounds 317–318 (2001) 497–502

Journal of ALLOYS AND COMPOUNDS

www.elsevier.com/locate/jallcom

Smith thermal analysis of selected Pr–Mg alloys

A. Saccone[a,*], D. Macciò[a], J.A.J. Robinson[b,1], F.H. Hayes[b], R. Ferro[a]

[a]*Dipartimento di Chimica e Chimica Industriale, Sezione di Chimica Inorganica e Metallurgia, Università di Genova, Via Dodecaneso 31, 16146 Genoa, Italy*

[b]*Materials Science Centre, University of Manchester and UMIST, Manchester, UK*

Abstract

The Smith thermal analysis has been used in the experimental investigation of several Pr–Mg alloys to achieve a better definition of some of the phase equilibria characteristic of the Pr–Mg system. This technique has several advantages with respect to conventional thermal analysis methods, even though it is more time consuming and it can be applied only to relatively narrow ranges of temperature in any one experiment. Solvus lines in the Pr-rich region and temperatures of the invariant reactions of the Mg-rich region of the Pr–Mg system were re-determined.

Keywords: Smith thermal analysis; Magnesium alloys; Rare earth alloys

1. Introduction

Differential thermal analysis (DTA) has been used as a standard experimental technique in alloy phase diagram studies for just over a hundred years. According to Pope and Judd [1]:

> *...there seems to be little doubt but that Le Chatelier can justly be regarded as the originator of the technique of DTA* (*in* 1887). *Nevertheless, because his method was not strictly differential, it lacked sensitivity. It was not until twelve years that Sir W.C. Roberts-Austen published a description of the apparatus which forms the essential basis of all modern differential thermal analysers.*

(see Ref. [2]). In DTA small temperature differences that arise between the alloy sample and an inert reference material in the same thermal enclosure, caused by heat absorption/evolution from phase changes during heating/cooling, are detected by a differential thermocouple and are used to determine phase boundary temperatures. In conventional DTA a pre-set constant heating or cooling rate is normally applied to a low thermal mass sample by means of a high thermal mass furnace. This enables temperature scans over many hundreds of degrees to be made routinely and the temperatures where phase boundaries and phase reactions occur to be determined conveniently. In 1940 Smith [3] proposed a new method of thermal analysis in which the temperature difference between the sample and the furnace wall is controlled rather than the heating or cooling rate itself. This method of control gives constant heat flow conditions enabling measurements of heat capacities and transformation enthalpies to be made. Using a low-thermal-mass furnace and a high-thermal-mass sample, enables thermal analysis to be carried out in which thermal events occurring within the sample itself essentially control the rate of change of temperature at any point in time. For example, when the temperature difference between the furnace and the sample is controlled, so that the furnace is hotter than the sample, then the sample will heat up over time. However, when the sample temperature reaches a value where an isothermal invariant phase reaction occurs, such as the melting point of a pure component or a eutectic reaction in a binary or ternary system, then the temperatures of both the sample and the furnace will remain constant until the reaction is completed before any further change in temperature occurs. Consequently, the entire sample is maintained in a state close to equilibrium throughout the heating process which gives the Smith method several advantages. For example it enables the temperatures of phase reactions and phase boundaries, separated by only a few degrees, to be determined. Even though the Smith method has been discussed on several occasions by different authors [4–8] it

*Corresponding author. Tel.: +39-010-3536-154.

E-mail address: saccone@chimica.unige.it (A. Saccone).

[1]Present address: NPL, Teddington, Middlesex, UK.

0925-8388/01/$ – see front matter
PII: S0925-8388(00)01377-3

has not found widespread use in phase diagram research, possibly because the equipment is not available commercially nor can conventional DTA be easily adapted to operate in the Smith mode. Over recent years the Smith method has been successfully applied to a variety of different alloy systems, Al-alloys [9–11], Au-alloys [9,12,13], In–Cd alloys [14].

In this paper we present the results obtained by applying the Smith method to some selected alloy compositions of the Pr–Mg system.

The systematics of the rare earth (R) alloys are of interest because they may be considered to be a tool for the investigation of the effects of the various elemental parameters on the alloying behaviour. By considering in fact a series of R–Me alloy (of different, mainly ''trivalent'' R with a metal Me) certain empirical regularities can be deduced (see, for instance, the general discussions presented on this topic by Gschneidner Jr. [15] and Colinet et al. [16]). In the specific case of the Mg alloys numerous R–Mg systems have been studied by using conventional analytical methods: Sc–Mg [17,18], Y–Mg [19,20], La–Mg [21,22], Ce–Mg [21,23], Pr–Mg [24], Nd–Mg [25], Sm–Mg [26], Eu–Mg [27], Gd–Mg [22,28], Tb–Mg [29], Dy–Mg [30], Ho–Mg [31], Er–Mg [32], Tm–Mg [33], Yb–Mg [34]. Several smooth trends have been observed to occur in the R–Mg series of compounds for different properties (compound formation, temperatures of the invariant equilibria, etc.) as functions of the atomic number of the rare earth element involved. These trends, moreover, have been satisfactorily used also to optimise data and to predict the phase equilibria in specific ternary systems (such as R–R′–Mg systems formed by Mg with two rare earth metals [20,35–38]).

The systems formed by Mg with the rare earth metals are also interesting from a technological point of view; in fact the effects of rare earth additions (either singly or in pairs) on the magnesium alloy properties (mechanical, properties at high temperature, casting characteristics, corrosion resistance, etc.) have been especially considered by many authors. See, for instance, books such as *ASM Handbook* [39,40] and *Structure and Properties of Nonferrous Alloys* [41].

A good definition of the characteristics of selected R–Mg systems may therefore be especially important. To this end a revision of certain complex regions of the R–Mg systems has been undertaken using the Smith technique in order to make a better evaluation of the invariant equilibria.

In this paper the modifications which have been performed on the classical Smith apparatus in order to be able to handle very reactive (and with high vapour pressure) alloys are presented. The results obtained for the Pr–Mg system with some Pr-rich and Mg-rich alloys (characterised by complex invariant equilibria close each to other) are discussed.

2. Pr–Mg system: literature data

The Pr–Mg alloy system was previously studied by the group at Genova University (Genoa, Italy) [24]. Formation of the following phases and invariant equilibria was suggested: PrMg (cubic, cP2, CsCl type, melting point 765°C), $PrMg_2$ (cubic, cF24, $MgCu_2$ type, peritectic formation 740°C), $PrMg_3$ (cubic, cF16, BiF_3 type, melting point 790°C), Pr_5Mg_{41} (tetragonal, tI92, Ce_5Mg_{41} type, peritectic formation 575°C) and $PrMg_{12}$ (tetragonal, tI26, $ThMn_{12}$ type, peritectic formation 565°C). $PrMg_2$ undergoes a eutectoidal decomposition at 670°C. Three eutectic reactions were observed to occur at 735°C and 40 at. % Mg, at 725°C and 59.5 at. % Mg and at 560°C and 95.0 at. % Mg. The (βPr) terminal solid solution was observed to decompose eutectoidally at 510°C and 19.5 at. % Mg.

3. Experimental

The main aim of this work was related to the use of the Smith technique. This is described below. To check the samples, however, several other experimental methods were employed, namely: X-ray powder diffraction, optical and scanning electron microscopy and electron probe microanalysis. Details of these techniques have been reported previously [24,30].

3.1. Smith thermal analysis: description of the equipment

A schematic drawing of the Smith thermal analysis rig is shown in Fig. 1a. The principal aim of its design is to have a variable heating and cooling rate furnace of low thermal inertia which is capable of responding quickly to abrupt changes in the rate of change of the sample temperature during heating and cooling runs. To achieve this, the vertical tube furnace is not lagged, but instead the furnace winding is simply surrounded by an air gap. The crucible materials and designs used vary according to the reactivity of the alloy samples being studied. Ideally, open crucibles should be used which enable samples to be stirred during heating and cooling runs through liquid/(liquid+solid) phase fields. However, the highly reactive nature of the Pr–Mg alloy samples used in the present work necessitated containing the samples in sealed crucibles made from tantalum. The design and dimensions of these crucibles are given in Fig. 1b. The tantalum crucible, containing about 1 g of alloy sample, is positioned vertically inside the central removable round-bottomed silica tube. The base of this silica tube rests on loosely packed ceramic wool contained inside the inner alumina tube, and is held vertically by a second open-ended silica tube surrounded by the ceramic wool. The ceramic wool permits argon gas to flow upwards through the furnace thereby preventing oxidation of the

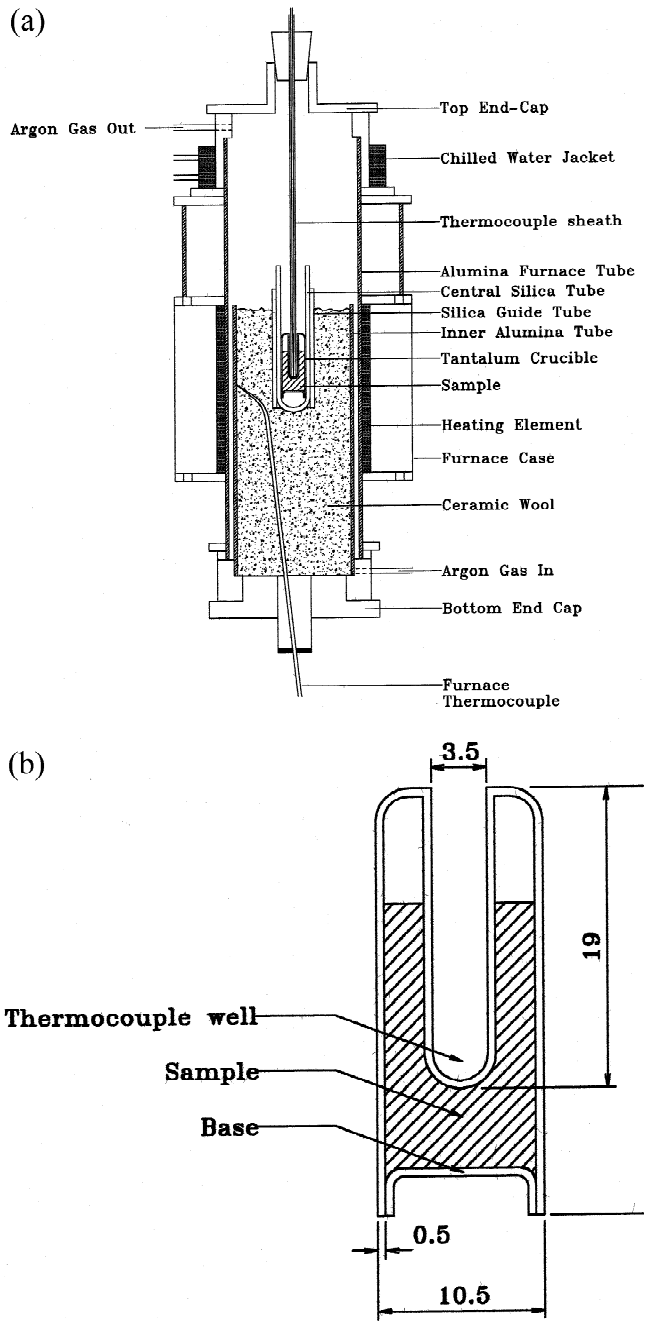

Fig. 1. (a) Schematic diagram of the Smith thermal analysis apparatus. (b) Welded tantalum crucible for the examination of reactive alloys in the Smith apparatus (dimensions in mm).

crucible during runs at elevated temperatures. The inner alumina tube rests, as shown, on the stainless steel bottom end-cap. The central silica tube containing the crucible is carefully positioned with respect to the furnace windings so that the sample is located centrally within the uniform temperature zone of the vertical tube furnace. The thermocouple junction used to measure the temperature of the sample is contained in a sealed alumina sheath which fits closely inside the thermocouple well of the crucible. The junction of this thermocouple also forms a differential thermocouple with a second thermocouple junction located at the inner wall of the furnace tube and lying in the same horizontal plane as the measurement couple. It is this differential thermocouple which enables the rig to be operated in the Smith mode. The signal from the differential thermocouple is sampled 50 times per second by a millivolt controller which adjusts the furnace power via a thyristor stack so as to maintain the thermocouple voltage as close as possible to the particular pre-set value. The thermocouple signal from the sample temperature measuring thermocouple is amplified, fed to a computer via an analog-to-digital converter and displayed on the monitor. The sample temperature is measured several times per second and the averaged value is printed out every 15 s alongside a continually up-dated plot showing mV and rate of change of temperature with time.

The thermocouple is calibrated by means of the melting points of pure metals, such as In, Sn, Bi, Pb, Zn, Al.

Examples of the Smith apparatus response for Pr–Mg alloys are shown in Fig. 2a and b.

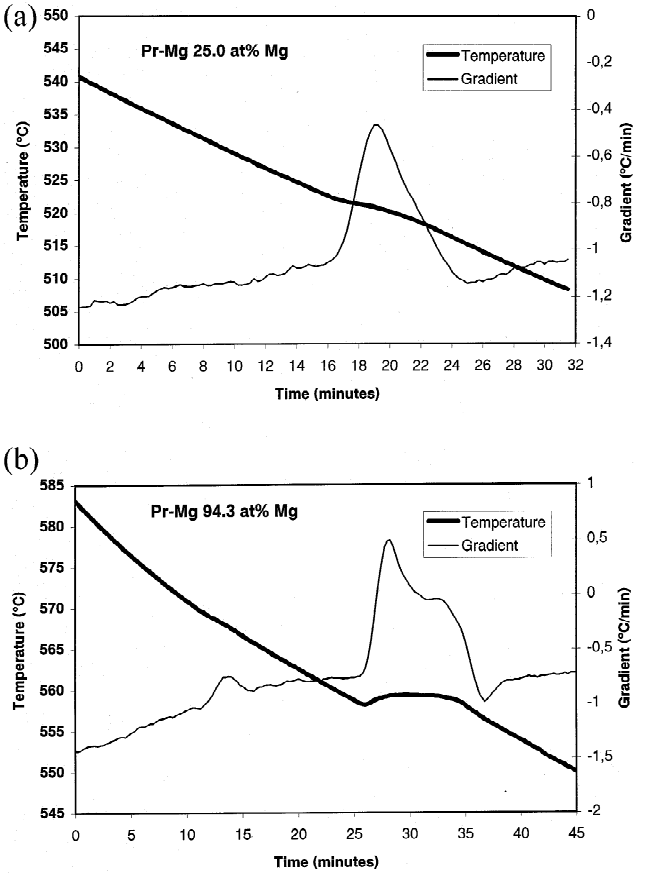

Fig. 2. Examples of Smith cooling traces for Pr–Mg alloys (only selected portions of the thermograms are reported). In the plots both the temperature (°C) and the rate of change of temperature (°C/min) versus time (min) are reported. (a) Pr–Mg, 25.0 at. % Mg. (b) Pr–Mg, 94.3 at. % Mg.

3.2. Sample preparation

Appropriate weighed amounts of Mg (99.99 mass % purity) and Pr (99.9 mass % purity), supplied by Koch Chemicals Ltd. (Hertford, UK), in small pieces were introduced into the open inverted tantalum crucibles and then sealed by Tungsten Inert Gas (TIG) welding the base to the body of the crucible under argon. When cool, the sealed crucibles were inverted once more so that the thermocouple well pointed upwards and, under flowing argon, heated in an induction furnace, to a temperature above the liquidus and held for some minutes. After mildly shaking the molten samples to homogenise, the alloys were immediately cooled down by switching off the furnace. The sealed crucibles were then studied by Smith thermal analysis. After completion of the thermal analysis, the samples were removed from their crucibles and studied by optical metallography, scanning electron microscopy, electron microprobe analysis and X-ray diffraction. A total of 12 Pr–Mg samples were studied by Smith thermal analysis. However three samples were subsequently found by Electron Probe MicroAnalysis (EPMA) to be highly segregated. Results for the remaining nine samples are reported below.

4. Results and discussion

The results obtained are shown in Fig. 3a and b where they are superimposed on the previously proposed Pr–Mg phase diagram [24]. A list of the alloys investigated is also reported in Table 1.

Two particular regions of the Pr–Mg phase diagram were studied in order to check both the solid state transformations and reactions and to examine the sequence of equilibria involving the liquid phase which lie very close to each other.

4.1. Pr-rich alloys

A satisfactory level of agreement exists between the data for the boundary curves of the (αPr) phase. The curve (αPr)/[(αPr)+PrMg] was accepted in our previous paper concerning the Pr–Mg phase diagram from Joseph and Gschneidner Jr. [42] who obtained it by lattice parameter measurements. The thermal analysis data obtained in the present work and relevant to the alloys at 5 and 7.5 at. % Mg are in very good agreement with this curve. The 7.5 at. % Mg alloy also gave a value relevant to the (αPr)/[(αPr)+(βPr)] curve, which was previously only estimated because it was not possible to obtain reliable data from the conventional DTA technique.

For the eutectoidal equilibrium (βPr)⇄(αPr)+PrMg fair agreement exists between the previous version and the new data (from the alloys at 22.0 and 25.0 at. % Mg). A slightly higher temperature (523°C instead of 510°C) was obtained for the invariant reaction.

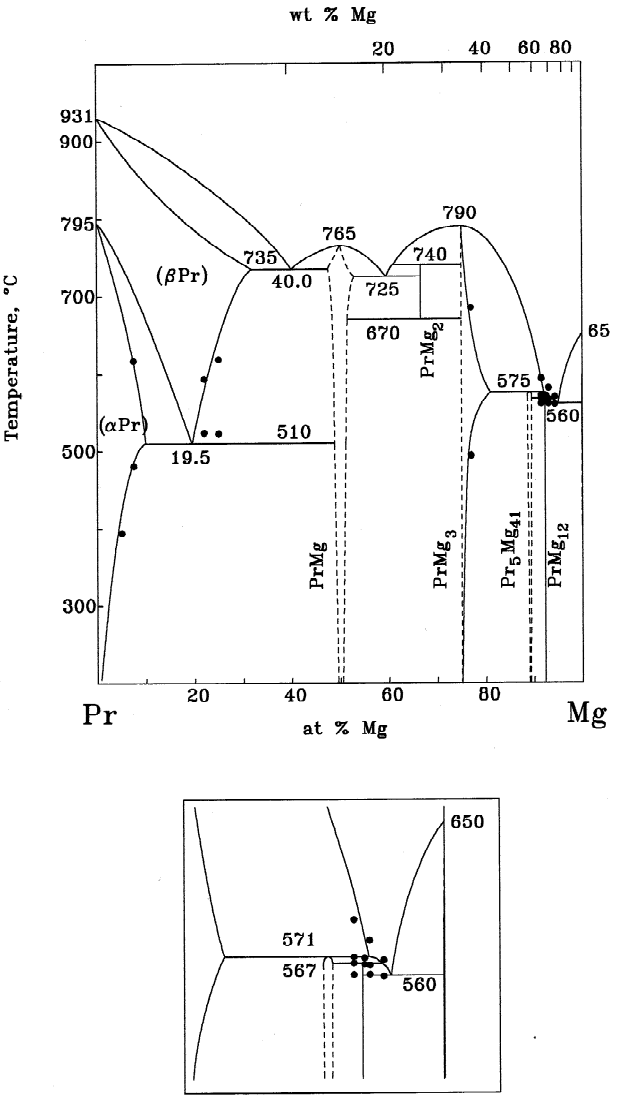

Fig. 3. (a) Phase diagram of the Pr–Mg system as obtained by Ref. [24]. The present Smith thermal analysis data are superimposed (black circles). (b) Enlarged Mg-rich region. The liquidus curve is slightly modified to better match the new thermal data.

4.2. Mg-rich alloys

One alloy (at 77 at. % Mg) was prepared in the region corresponding to the homogeneity range of the $PrMg_3$ phase. The Smith thermal data confirms the wide solubility range previously attributed to the $PrMg_3$ phase only on the basis of its lattice parameter trend and of the micrographic appearance of the samples prepared around its stoichiometric composition.

Four alloys richer in Mg (91.5, 92.5, 93.0 and 94.3 at. % Mg) were prepared to check the equilibria involving the phases with the highest Mg content [Pr_5Mg_{41}, $PrMg_{12}$ and

Table 1
Selected Pr-rich and Mg-rich alloys prepared and analysed by Smith thermal method

Nominal composition (at. % Mg)	Thermal effects[a] (°C)	Micrographic appearance and EPM analysis	X-Ray powder diffraction lines
5.0	395	(Pr)	(αPr)
7.5	481; 617	(Pr) + small quantities of (βPr) showing complete eutectoidal decomposition	(αPr) + PrMg
22.0	524; 593	PrMg + of (βPr) showing complete eutectoidal decomposition	PrMg + (αPr)
25.0	523; 619	PrMg + (βPr) showing complete eutectoidal decomposition	PrMg + (αPr)
77.0	494; 685	$PrMg_3$	$PrMg_3$
91.5	560; 567; 571; 593 (L)	Pr_5Mg_{41} + $PrMg_{12}$ + eutectic [$PrMg_{12}$ + (Mg)]	Pr_5Mg_{41} + $PrMg_{12}$ + (Mg)
92.5	567; 570	$PrMg_{12}$ + eutectic [$PrMg_{12}$ + (Mg)]	$PrMg_{12}$ + (Mg)
93.0	561; 566; 581 (L)	$PrMg_{12}$ + eutectic [$PrMg_{12}$ + (Mg)]	$PrMg_{12}$ + (Mg)
94.3	560; 569 (L)	$PrMg_{12}$ + eutectic [$PrMg_{12}$ + (Mg)]	$PrMg_{12}$ + (Mg)

[a] Averaged values among the heating and cooling runs.
L = Liquidus point.

(Mg)]. For these various equilibria (in comparison with the previous data) the following values were observed:

$L + PrMg_3 \rightleftarrows Pr_5Mg_{41}$ at 571°C (instead of 575°C)

$L + Pr_5Mg_{41} \rightleftarrows PrMg_{12}$ at 567°C (instead of 565°C)

$L \rightleftarrows PrMg_{12} + (Mg)$ at 560°C (same value)

The data for the liquidus suggest a slightly different trend in the liquidus curve with respect to the previously proposed version of the Pr–Mg phase diagram. The liquidus compositions for the peritectic reactions of formation of the two Mg-rich phases Pr_5Mg_{41} and $PrMg_{12}$ are suggested to be about 93 and 94 at. % Mg, respectively.

The X-ray and micrographic analyses carried out on all the samples were in agreement with the phase equilibria summarised in Fig. 3a and b.

Examples of photomicrographs both of Pr-rich and Mg-rich alloys are shown in Figs. 4 and 5.

4.3. General remarks

At first we may remark that the Pr–Mg phase diagram has been confirmed and better defined in some specific regions.

As for the Smith technique, it proved to be a valuable method, particularly in detecting those solid state transformations in which very weak thermal effects are involved. It is also useful in separating effects close to each other and prone to overlap in conventional DTA methods.

Moreover, the use of samples closed in tightly welded sealed crucibles allows the satisfactory application of this technique to the analysis of very reactive samples, such as rare earth alloys, and/or having high vapour pressure, such as Mg and its alloys.

To this end, the analysis of other binary and ternary alloys of Mg with rare earths is in progress.

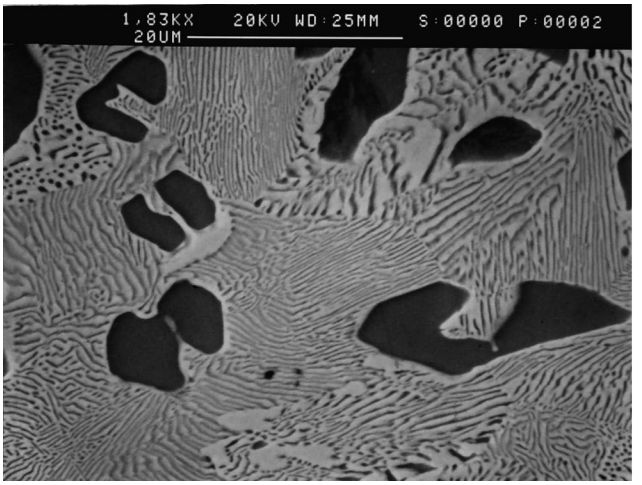

Fig. 4. Backscatter electron (BSE) micrograph of a Pr–25 at. % Mg (as obtained after the Smith thermal analysis runs). PrMg grains (black) surrounded by (βPr) that shows a complete eutectoidal decomposition into lamellar PrMg and (Pr).

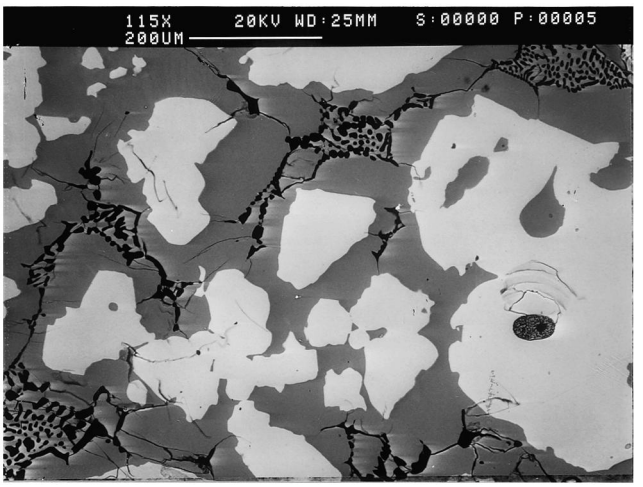

Fig. 5. Backscatter electron (BSE) micrograph of a Pr–91.5 at. % Mg (as obtained after the Smith thermal analysis runs). Pr_5Mg_{41} (white) surrounded by $PrMg_{12}$ (grey) and eutectic formed by $PrMg_{12}$ and (Mg).

Acknowledgements

This work is performed in the framework of the Italian ''Programmi di Ricerca Scientifica di Rilevante Interesse Nazionale'' of the MURST (Ministero dell'Università e della Ricerca Scientifica e Tecnologica) and of the Italian Progetto Finalizzato ''Materiali Speciali per Tecnologie Avanzate II'' (PF MSTA II), whose support are gratefully acknowledged. D.M. and F.H.H. are grateful to the ''British Council'' for fellowships in Manchester and Genoa, respectively. This exchange program has provided the starting activity in the early stage of this research co-operation.

References

[1] M.I. Pope, M.D. Judd, Differential Thermal Analysis – A Guide to the Technique and Its Applications, Heyden, 1977.
[2] W.C. Roberts-Austen, Proc. Inst. Mech. Eng. 1 (1899) 35.
[3] C.S. Smith, Trans. Am. Inst. Mining Metall. Eng. 137 (1940) 236.
[4] W. Hume-Rothery, J.W. Christian, W.B. Pearson, in: Metallurgical Equilibrium Diagrams, Institute of Physics, London, 1956, p. 126.
[5] W. Hume-Rothery, J.W. Christian, W.B. Pearson, in: Metallurgical Equilibrium Diagrams, Institute of Physics, London, 1956, p. 130.
[6] F.N. Rhines, in: Phase Diagrams in Metallurgy – Their Development and Application, McGraw-Hill, 1956, pp. 301–302.
[7] G.V. Raynor, Phase diagrams and their determination, in: R.W. Cahn (Ed.), Physical Metallurgy, 2nd Edition, North Holland, Amsterdam, London, 1970.
[8] E.E. Sidorova, L.G. Berg, in: R.C. Mackenzie (Ed.), Differential Thermal Analysis, Vol. 2, Academic Press, London, 1972, pp. 11–12, Chapter 26.
[9] F.H. Hayes, W.T. Chao, Purple plague and the Al–Au–Si system, in: User Aspects of Phase Diagrams, Institute of Metals, London, 1991, pp. 121–127.
[10] F.H. Hayes, R.D. Longbottom, E. Ahmed, G. Chen, J. Phase Equilibria 14 (1993) 425.
[11] F. Weitzer, P. Rogl, F.H. Hayes, J.A.J. Robinson, Phase relations in the Al-rich part of the system: Al–Fe–Mn, in: F. Aldinger, H. Murghrabi (Eds.), Werkstoff Woche'95, Materialwissenschaftliche Grundlagen, Deutsch Gesellschaft für Materialkunde, Frankfurt, 1997, pp. 185–190.
[12] F.H. Hayes, J.A.J. Robinson, W.T. Chao, Application of Smith thermal analysis to ternary systems of interest in joining processes in solid state device technology, in: J.E. Morral, R.S. Schiffman, S.M. Merchant (Eds.), Experimental Methods of Phase Diagram Determination, TMS, Warrendale, PA, 1994, pp. 101–111.
[13] F.H. Hayes, W.T. Chao, J.A.J. Robinson, J. Thermal Anal. 42 (1994) 745.
[14] P.J. Horrocks, F.H. Hayes, N.D. Moulson, Thermochim. Acta 204 (1992) 25.
[15] K.A. Gschneidner Jr., J. Less-Common Metals 17 (1969) 1.
[16] C. Colinet, A. Pasturel, A. Percheron-Guegan, J. Less-Common Metals 102 (1984) 167.
[17] L.N. Komissarova, B.I. Pokrovskii, Russ. J. Inorg. Chem. 9 (10) (1964) 1233.
[18] A. Pisch, R. Schmid-Fetzer, G. Cacciamani, P. Riani, A. Saccone, R. Ferro, Z. Metallkd. 89 (1998) 474.
[19] E.D. Gibson, O.N. Carlson, Trans. ASM 52 (1960) 1084.
[20] M. Giovannini, A. Saccone, R. Marazza, R. Ferro, Metall. Mater. Trans. A 26A (1995) 5.
[21] R. Vogel, T. Heumann, Z. Metallkd. 38 (1947) 1.
[22] P. Manfrinetti, K.A. Gschneidner Jr., J. Less-Common Metals 123 (1986) 267.
[23] A.A. Nayeb-Hashemi, J.B. Clark, Phase Diagrams of Binary Magnesium Alloys, ASM International, Metals Park, OH, 1988.
[24] A. Saccone, A.M. Cardinale, S. Delfino, R. Ferro, Intermetallics 1 (1993) 151.
[25] S. Delfino, A. Saccone, R. Ferro, Metall. Trans. A 21 (1990) 2109.
[26] A. Saccone, S. Delfino, G. Borzone, R. Ferro, J. Less-Common Metals 154 (1989) 47.
[27] W. Mühlpfordt, W. Klemm, J. Less-Common Metals 17 (1969) 127.
[28] G. Cacciamani, A. Saccone, G. Borzone, S. Delfino, R. Ferro, Thermochim. Acta 199 (1992) 17.
[29] A. Saccone, S. Delfino, D. Macciò, R. Ferro, J. Phase Equilibria 14 (1993) 479.
[30] A. Saccone, S. Delfino, D. Macciò, R. Ferro, Z. Metallkd. 82 (1991) 568.
[31] A. Saccone, S. Delfino, D. Macciò, R. Ferro, J. Phase Equilibria 14 (1993) 280.
[32] A. Saccone, S. Delfino, D. Macciò, R. Ferro, Metall. Trans. A 23 (1992) 1005.
[33] A. Saccone, D. Macciò, S. Delfino, R. Ferro, J. Alloys Comp. 220 (1995) 161.
[34] O.D. McMasters, K.A. Gschneidner Jr., J. Less-Common Metals 8 (1965) 289.
[35] M. Giovannini, A. Saccone, R. Ferro, J. Alloys Comp. 220 (1995) 167.
[36] H. Flandorfer, M. Giovannini, A. Saccone, P. Rogl, R. Ferro, Metall. Mat. Trans. A 28A (1997) 265.
[37] M. Giovannini, A. Saccone, H. Flandorfer, P. Rogl, R. Ferro, Z. Metallkd. 88 (1997) 372.
[38] M. Giovannini, A. Saccone, R. Ferro, Intermetallics 7 (1999) 909.
[39] K.A. Gschneidner Jr., B.J. Beaudry, J. Capellen, Rare earth metals, in: ASM Handbook, Properties and Selection: Nonferrous Alloys and Special-Purpose Materials, Vol. 2, ASM International, Materials Park, OH, 1990, pp. 720–732.
[40] S. Housh, B. Mikucki, A. Stevenson, Selection and application of magnesium and magnesium alloys, in: ASM Handbook, Properties and Selection: Nonferrous Alloys and Special-Purpose Materials, Vol. 2, ASM International, Materials Park, OH, 1990, pp. 455–516.
[41] G. Neite, K. Kubota, K. Higashi, F. Hehmann, Magnesium-based alloys, in: R.W. Cahn, P. Haasen, E.J. Kramer (Eds.), Materials Science and Technology. A Comprehensive Treatment, Structure and Properties of Nonferrous Alloys, Vol. 8, VCH, Weinheim, 1996, pp. 113–212, K.H. Matucha (volume editor).
[42] R.R. Joseph, K.A. Gschneidner Jr., Trans. Metall. Soc. AIME 233 (1965) 2063.